Nautilus: Robust, positivity and divergence preserving code for multi-fluid, multi-species electromagnetics and plasma physics applications*

Ammar H. Hakim† and John Loverich*

I. Background

In this paper we will present algorithms implemented in Nautilus, a new code for the solution of a wide variety of plasma and neutral fluid equations. Nautilus can simulate fully and weakly ionized flows and has been applied to fast magnetohydrodynamics (MHD) devices like Z-pinches and dense-plasma focuses, chemically reacting hypersonic flows and plasma jet propagation and merging for the creation of high energy-density states in the laboratory. We present details of new positivity preserving fluid algorithms as well as collocated Maxwell equation solvers that preserve divergence and work on general geometries. Current state of Nautilus is described and future directions outlined.

II. Introduction

The dynamical behavior of plasmas is strongly dependent on frequency. At the lowest frequency the plasma is in the regime of magnetohydrodynamics (MHD) and has been the focus of extensive research in fluid plasma modeling in the past few decades. Efficient schemes, in particular, based on semi-implicit methods,[3] have been developed for resistive MHD. More recently, schemes to take into account Hall-currents and magnetic drifts have also been developed. Production quality codes like NIMROD[12] implement enhanced versions of these schemes and are being applied to extended MHD simulations of tokamaks and other fusion devices. At somewhat higher frequencies, the electrons and ions can move relative to each other, behaving like two charge separated, interpenetrating fluids. This is the regime of high-frequency, non-neutral two-fluid physics and is relevant to high-density, fast MHD phenomena encountered in pulsed-power devices like dense plasma focus, Z-pinches, plasma thrusters and field-reversed configurations. Although initial work has been done on efficiently solving fast MHD phenomena, several open research problems remain. For example, implicit schemes developed for application in slow MHD can not be applied directly as pulsed-power devices commonly exhibit shocks and other sharp features in the flow. Two-fluid equations can also be made to include certain kinetic effects by solving for the pressure-tensor (and higher moments) self-consistently and by using several fluid components per species. However, the inclusion of collisional effects and closure of the system is poorly understood. Another field of interest is to the modeling of weakly ionized plasmas in hypersonic flows. In this, the plasma sheath structure and the propagation of electromagnetic waves through the sheath needs to be studied. Additionally, plasma chemistry must to be included to capture the proper heat transfer among various components of the gas.

There are some existing codes that are used by researchers in pulsed power applications. In particular, MACH2 and MACH3 are, respectively, two-dimensional axisymmetric and three-dimension resistive MHD codes that are widely used. Options for including Hall terms are available. MACH2 is essentially a serial code but some parallel versions, scaling to several processors, are available. MACH2/3 use arbitrary Lagrangian/Eulerian (ALE) algorithms for solution of the fluid equations. These schemes are not shock capturing and frequently lead to mesh entanglement from grid motion. Further, advanced fluid closures, to simulate certain kinetic effects, are not presently included and would be difficult to add. A disadvantage of these codes is the lack of wide availability outside the Air-Force Research Laboratories. For example, students working on pulsed power devices have limited access and support for these codes, specially to MACH3. Further, these codes are not easily extensible for applications to other domains of interest.

*Submitted to 41st AIAA Plasmadynamics and Lasers Conference

†Tech-X Corporation, 5621, Arapahoe Avenue Suite A, Boulder, CO. 80303. (303)-444-2451

The situation should be contrasted to electromagnetic Particle-In-Cell (PIC) codes. There are several highly robust, parallel and widely available EM PIC codes, for example, VORPAL[a] and ICEPIC. VORPAL is available as a commercial product and is continuously enhanced and extensively supported and maintained with frequent new releases. Both VORPAL and ICEPIC have been applied to a wide variety of problems, specially for the simulation of high-power microwave tubes. These codes can simulated very complex geometries and incorporate a variety of plasma processes, including atomic physics and surface effects, including sputtering and field induced emission. Analogous codes in the domain of fluid plasma modelling are not available.

Hence, extensive research is required to develop widely available, production quality fluid modelling software that allows engineers, experimentalists, students and other researchers to model the enormous range of frequencies and configurations of interest to a wide variety of engineers and scientist. `Nautilus` aims to fill in this gap by providing a widely available and commercially supported plasma fluids code that is flexible, easy to use and applicable to a broad range of problems.

III. Overview of Nautilus

Nautilus is a flexible and parallel code for solving a variety of fluid equations in general geometries. The presently supported models in Nautilus are an electromagnetic two-fluid five-moment (number density, momentum and pressure) model, an electromagnetic two-fluid ten-moment (number density, momentum and pressure tensor) model, resistive and Hall-MHD models and neutral viscous, compressible flow models. In addition, an electrostatic Poisson solver and a Maxwell equation solver are implemented. All the above solvers work on structured body-fitted grids and unstructured grids. Although the structured grid algorithms work in parallel, unstructured grid algorithms presently work only in serial but parallel decomposition is planned as a part of current research. Two major families of shock-capturing algorithms, finite-volume and finite-element methods, are implemented. In the finite-volume family a high-resolution wave propagation algorithm and a MUSCL scheme[8] are implemented, while in the finite-element family an initial implementation of discontinuous Galerekin[9] algorithm is completed. The algorithms and plasma models are completely independent and can be combined in an arbitrary manner in input files. Additional solvers can be added to the code and "plugged into" a input file to construct a new simulation in combination with existing solvers. Presently only explicit schemes are implemented for solving the fluid equations. Further, simple fluid closure schemes are used in the two-fluid five- and ten-moment models and vacuum-plasma interfaces are not captured self-consistently, specially in the resistive and Hall-MHD models.

Some of the other key features of Nautilus are listed below

- Nautilus is highly modular, parallel, finite-volume and finite-element shock-capturing code supporting both structured and unstructured meshes.
- Nautilus uses novel stable and accurate algorithms to capture fluid-vacuum interfaces for the neutral fluid and resistive MHD equations. These have been used to study jet propagation and merging in vacuum.
- Nautilus has simple radiation loss models that have been used to study the effect of radiation, in the optically thin limit, on pressure gain in an inertial confinement fusion experiment.
- An extensive infrastructure for computing synthetic diagnostics is implemented in Nautilus. These allow computing integrated quantities like mass and energy, recording fields as specified locations in the domain, computing peak pressure, plasma currents, inductance, capacitance and electric potentials. Other diagnostics can be easily added and used in existing simulations.

In the next subsection we describe applications of Nautilus which demonstrate the above features in production quality simulations.

IV. Self Consistent Coupled Simulations of Field Reversed Configurations

Fusion promises to be an efficient mechanism for the generation of clean energy. An objective of fusion research is the application of fusion energy in a manner acceptable to society. This concerns not only its economic benefit, but also safety and environmental issues. A number of fusion devices are currently under investigation and can be classified into two broad classes based on the device geometry. The first, and more rigorously studied and funded, is the class

[a]See http://www.txcorp.com/products/VORPAL/index.php for a product overview of VORPAL

of toroids (donut shaped devices). ITER (`http://www.iter.org/`) is an example of a international collaboration on building a facility to produce fusion power using toroidal devices. The device is expected to produce power by 2015. The other class of fusion devices are the *compact toroids* with cylindrical geometry and are also actively under investigation for use in fusion power reactors.

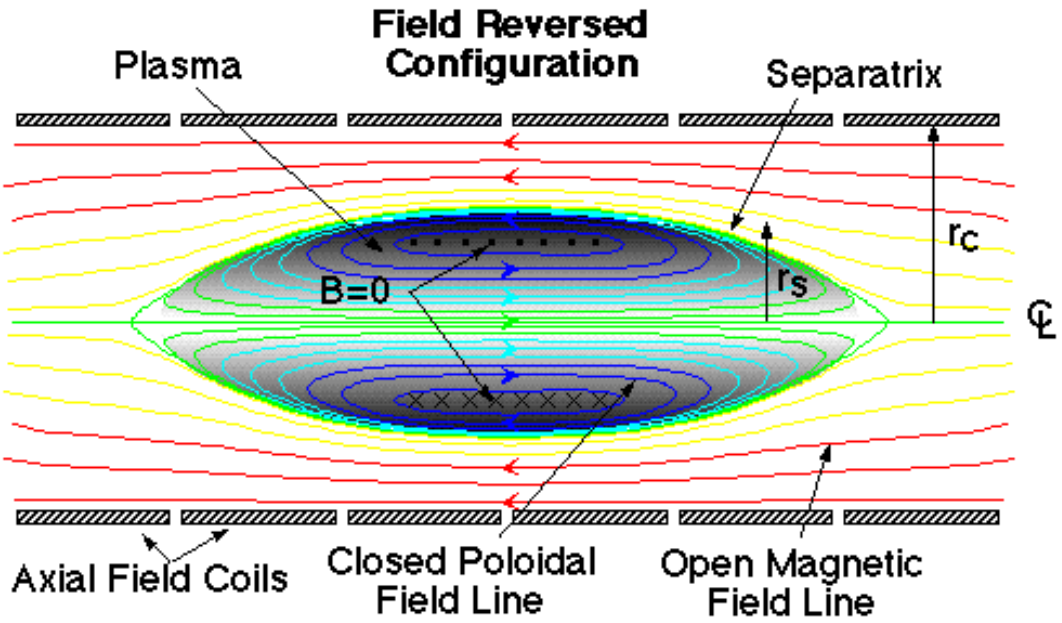

Figure 1. Schematic diagram of a Field Reversed Configuration. The device is cylindrical and a $r-z$ plane slice through the axis is shown.

The Field Reversed Configuration (FRC) and Spheromak[1] belong to the family of compact toroids. These devices do not have any internal material structures ("compact") allowing the plasma to extend to the device axis. The magnetic field topology is that of a closed donut-shaped surface ("toroidal"). Figure 1 shows a schematic diagram of an FRC.

It is known that Two–Fluid effects play an important role in FRC physics. Two fluid formalism to study FRC stability[7,14,15,17,18] has been extensively developed. Relaxation of Two–Fluid equlibria has also been studied.[13] However no detailed numerical studies of FRCs using the Two–Fluid model have been performed before although some results have been obtained using particle simulations.[2]

In this section we describe the self-consistent coupled simulations of the FRC formation using theta-pinch coils.

The first set of simulations we have coupled theta-pinch coils to the two-fluid plasma solver to perform self-consistent EM-fluid simulations of the FRC formation dynamics. The domain was a cylinder tube 50 cms long by 10 cm radius. Two sets of coils were put into the domain. The magnetic field from these coils was computed self-consistently, given the current profiles. Note, however, that the back reaction of the plasma on the theta-pinch circuits was not taken into account. The central theta-pinch coil was 36 cm long and was placed at a radius of 7 cm. The mirror coils were 10 cm long each, with a 2 cm gap between the theta-pinch coils and the mirror coils. The mirror coils were also placed at the same radius as the theta-pinch coils. In the experiment this is not the case, the mirror coils being closer than the theta-pinch coils.

Constant current was run through the mirror coils, while the theta-pinch coils had a current profile which gave an initial bias field of about -0.4 Tesla. See Fig. 2 for details. Once an equilibrium magnetic field was calculated a Deuterium plasma with number density $1\times10^{22}\ m^{-3}$ was introduced. Note that this is 10× larger than used in the first problem described above. Once the magnetic field froze into the plasma, the theta-pinch coil currents were reversed. For this a hyperbolic tangent current profile was used which reversed the field on a time scale of about a tenth of a micro-second. The peak axial field after reversal was about 3.0 Tesla.

The next set of simulations were performed to make sure our two-fluid solver has the physics needed to model FRC formation. The simulation parameters were selected to be less stringent than in the MTF experiment for this initial case. True parameters were used in the second problem described below. The domain was a quartz tube 50 cms long by 6.2 cm radius. A constant axial magnetic field of 1.0 Tesla was applied to the wall. The domain was filled with a Deuterium plasma with number density $1\times10^{21}\ m^{-3}$ for both electrons and ions. A bias axial field of -0.2 Tesla was frozen into the plasma. The initial pressure was selected to give plasma beta ($p/(B^2/2\mu_0)$) of unity, computed from the

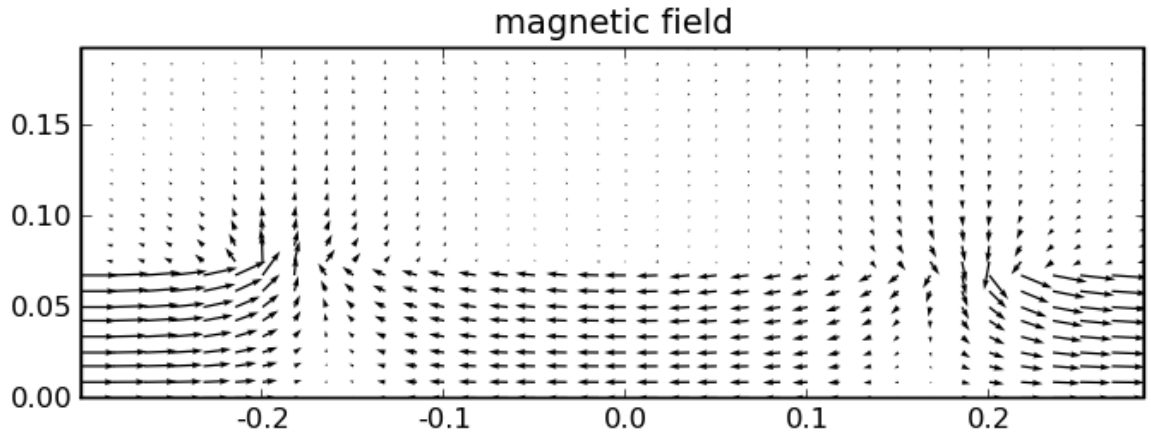

Figure 2. Equilibrium magnetic field stream lines produced by a set of theta-pinch and mirror coils (not shown). Note the structure of the initial magnetic field which allows for the trapping of magnetic flux in the FRC during formation. The peak bias axial field is about -0.4 Tesla. After reversal the peak axial field is about 3.0 Tesla.

bias field. The plasma fill was only initialized in a region of axial length 36 cm and radius 3.1 cms. The solution was evolved using the full two-fluid equations and algorithms previously developed by us and described in.[4–6,9,11] For this problem we did not use the coil magnetic fields but simply held the wall axial magnetic field constant.

The FRC formation was seen to occur very rapidly. The initial plasma "cylinder" collapsed to the axis in a few tenths of a microsecond as the wall field pushed the plasma towards the axis. When the plasma fluid pressure was sufficient the plasma bounced back, the field lines reconnected, and an FRC was formed. The reconnection drove a new radial contraction phase which was followed by an axial contraction of the plasma, till the FRC reached a quasi-equilibrium state. This occurred at about 2 μsec into the simulation. See Figs. 3 and 4 for the quasi-equilibrium FRC number densities and temperatures at 4 μsec.

Although in ideal-MHD theory FRCs do posses any toroidal fields, such fields are observed in FRC formation experiments.[10,16] In our simulations we have confirmed this. See Fig. 5 for a plot of the toroidal field. As the formation process is symmetric about the FRC mid-plane the net toroidal flux, as is evident from this plot, is zero. A non-zero flux should result when using conical theta-pinch coils as discussed by Wira.[16] The toroidal field is quite significant (1/10 of the poloidal field) at 4 μsecs but decays with time.

We have also investigated the electron currents which produce these toroidal fields. See Fig. 6 for an stream-function plot of the poloidal electron momentum. The plot shows the counter rotating rings of electron currents which sustain the toroidal fields. The decay of the toroidal fields with time indicates a decay of the poloidal electron moment, the energy possibly being transferred to the ions, which would explain the higher ion temperatures as seen in Fig. 4.

In the third set of simulations we have coupled theta-pinch coils (described above) to the plasma solver to perform self-consistent EM-fluid simulations of the FRC formation dynamics. As in the second set of simulations, the FRC formation was seen to occur very rapidly. After compression the field lines reconnect and the FRC forms in about 2 μsecs after field reversal in the theta-pinch coils. The FRC forms and compresses first radially and then axially to give a peak number density of 5×10^{22}. See Fig. 7 for a plot of the plasma number density. Fig. 8 shows the poloidal magnetic field structure after formation. This plot shows the expected closed field-line topology of the FRC poloidal field, indicating FRC formation was successful.

V. Two-Fluid Field Reversed Configuration Equilibria

In this set of simulations we have studied the relaxation of an ideal-MHD FRC equilibrium to a two-fluid equilibrium. The motivation for studying this problem is that the structure of FRC equilibrium in the two-fluid model is not well understood. To our knowledge the only two-fluid equilibrium solver is written by Loren Steinhauer[13,14] and uses a fixed boundary. The problem of self consistently determining the plasma equilibrium profile and separatrix shape is a crucial one if one is to attempt shaping of the equilibrium FRC plasma using coil currents. Such shaping is done on

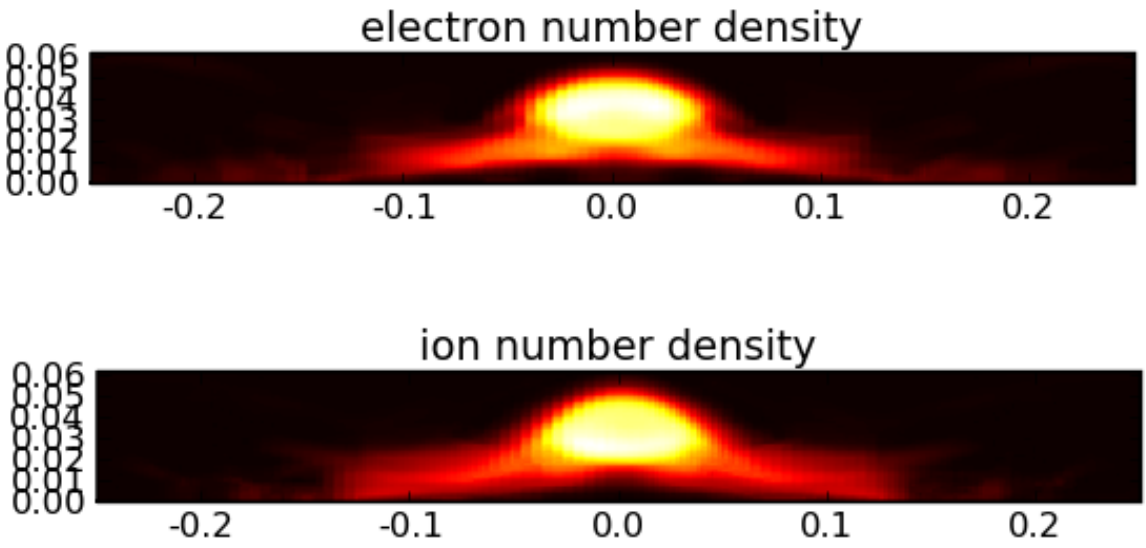

Figure 3. Electron (top) and ion (bottom) number densities at 4 μsec. The color scheme is selected to show 5×10^{21} m^{-3} for the brightest color. The FRC has formed and settled into a quasi-equilibrium state. The formation process is explosive: the initial plasma fill collapses to the axis on sub-microsecond scales and the field lines reconnect initiating an FRC. The FRC then contracts axially and reaches a peak density of 5×10^{21} m^{-3}.

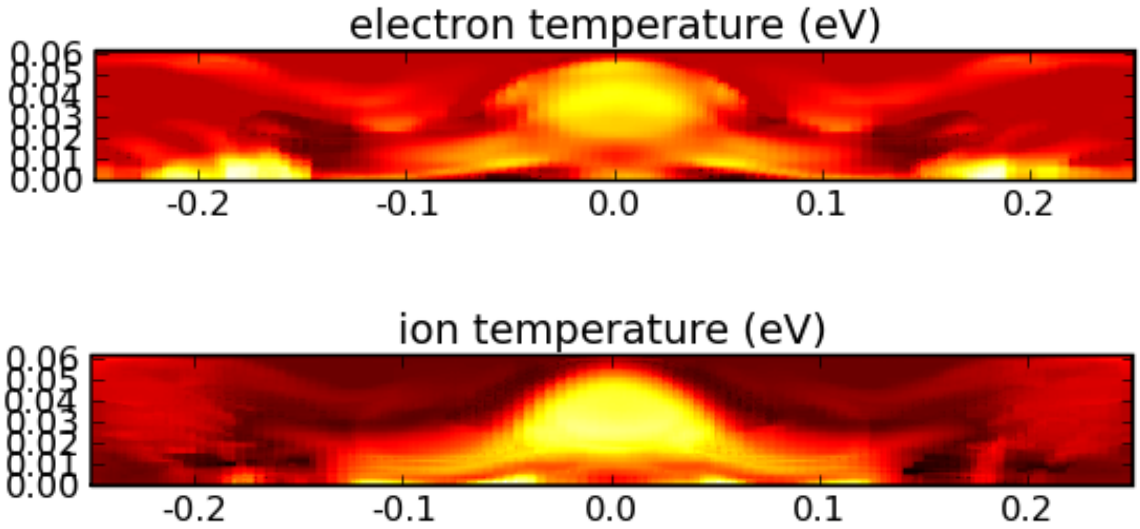

Figure 4. Electron (top) and ion (bottom) number densities at 4 μsec. The color scheme is selected to show 225 eV for the brightest color for the electrons and 400 eV for the ions. In this simulation the ions are hotter than the electrons, clearly showing two-temperature effects, which can not be captured in a single temperature MHD model.

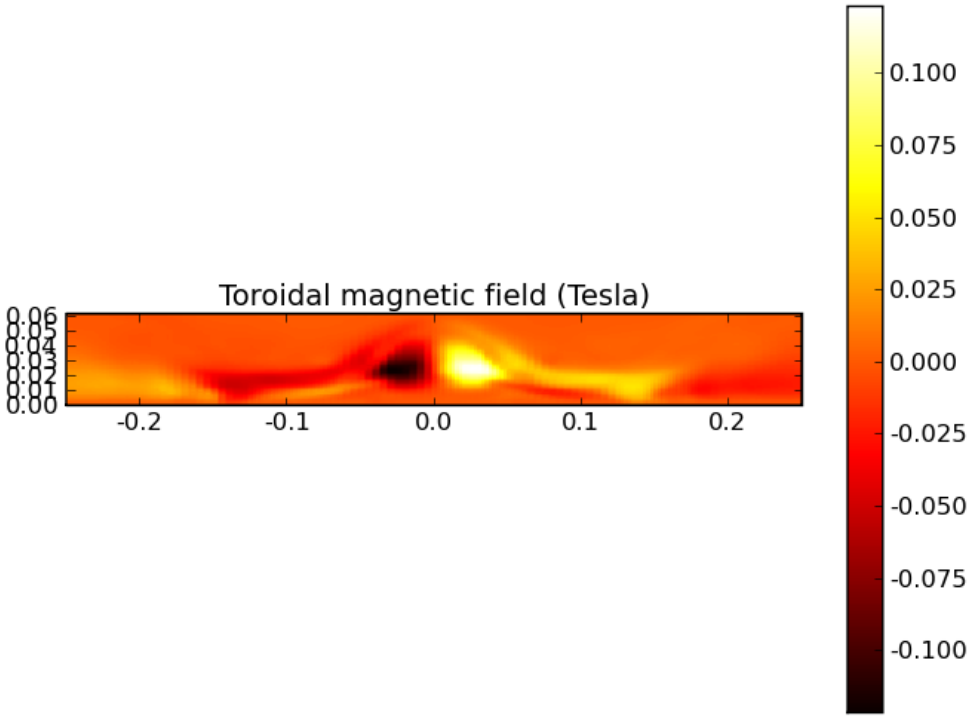

Figure 5. Toroidal magnetic field at 4 μsec. In ideal-MHD theory toroidal field is zero. However, such fields are observed in experiments. As the formation process is symmetric about the FRC mid-plane, the net toroidal flux is zero.

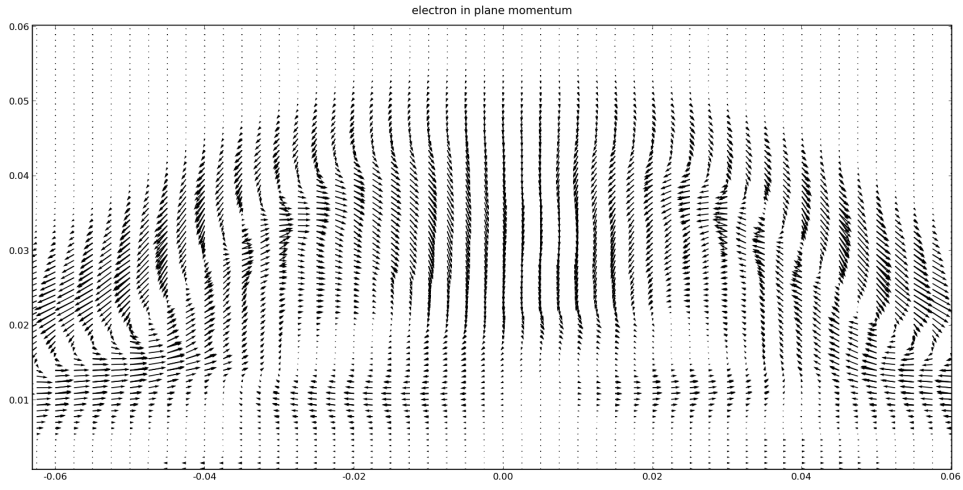

Figure 6. Polodial electron momentum at 4 μsec. The electrons rotate in the poloidal plane which generates the dipole toroidal magnetic fields seen in Fig. 5. The gradual decay of the electron poloidal moment could be the cause of ion heating seen by comparing with Fig. 4.

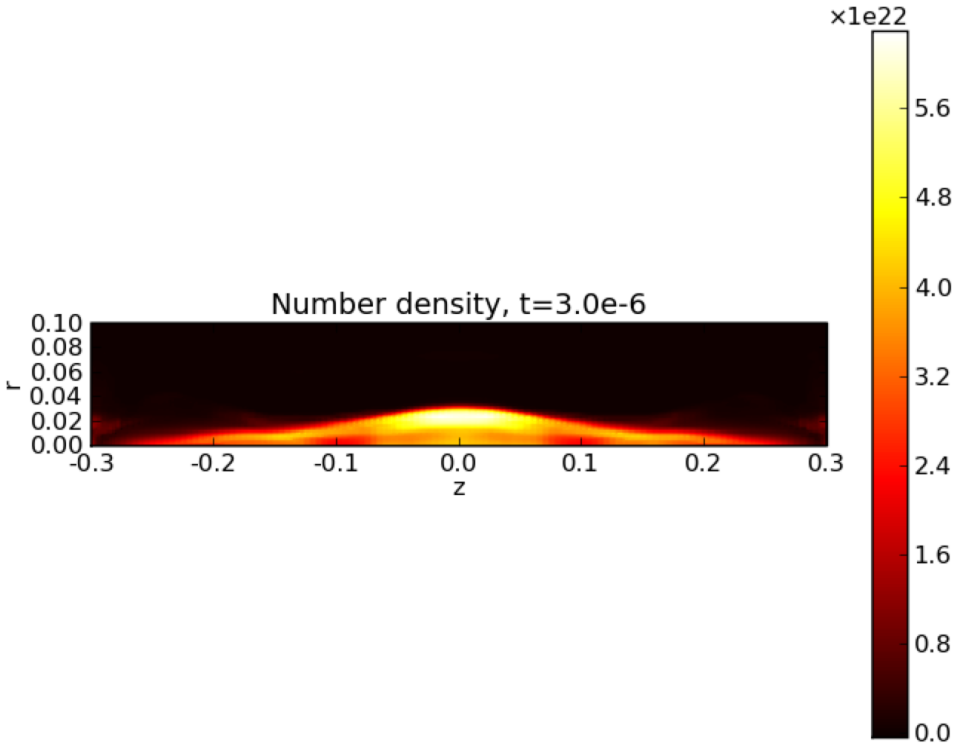

Figure 7. Plasma number density after FRC formation. The FRC has undergone radial and axial contraction and has achieved a peak number density of about $5 \times 10^{22}\ m^{-3}$. This occurs about 2 μsec after the current reverses in the theta-pinch coils.

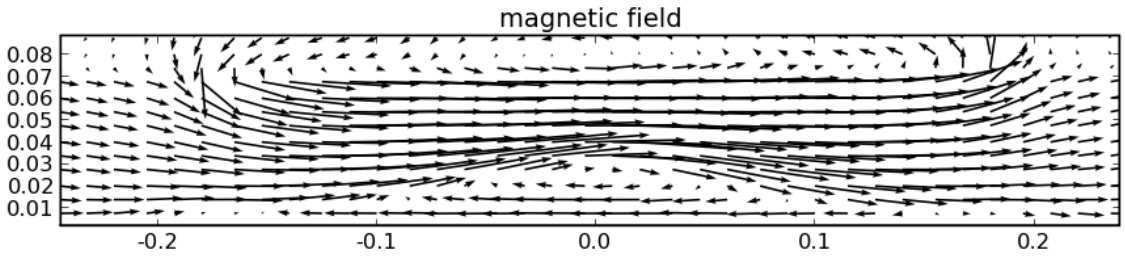

Figure 8. Poloidal magnetic field structure after FRC formation. This plot shows the expected closed field-line topology of the FRC poloidal field, indicating formation was successful. When the FRC is fully formed the current in the theta-pinch coils are reversed with respect to the initial bias field as seen from Fig. 2.

a regular basis for tokamaks with excellent results.

For this problem we have initialized the simulation with a rigid rotor equilibrium. This equilibrium is described by the flux function, $\psi(r, z)$, given by

$$\psi = -\frac{B_0}{2} r^2 \left(1 - \frac{r^2}{a^2} - \frac{z^2}{b}\right) \tag{1}$$

where $\psi = 0$ on the ellipse $r^2/a^2 + z^2/b = 1$. The initial magnetic field is in the poloidal plane and is given by $\mathbf{B}_p = \nabla\psi \times \mathbf{e}_\theta / r$, where $\mathbf{e}_\theta$ is a unit vector in the toroidal direction. The pressure profile can be found by the relation $p = -Cr/\mu_0$, where the Grad-Shafranov equation $\triangle_* \psi = -\mu_0 r^2 dp/d\psi$ can be used to determine C. This rigid rotor equilibrium is an exact solution of the ideal-MHD equations.

The domain was selected to be 6 cm in radius and 30 cm in length. The FRC seperatrix radius was selected to be 4 cm at the mid-plane. An aspect ratio of 5 was selected, giving an initial 20 cm long FRC. The nominal density was selected to be $1 \times 10^{22}\ m^{-3}$, and the two-fluid equations evolved. Although this initial condition is an ideal-MHD equilibrium, it is not a two-fluid equilibrium. Hence, the initial conditions eventually relax to a new two-fluid equilibrium. This two-fluid relaxation process involves a significant axial contraction. This contraction also causes toroidal electron currents which lead to a dipole toroidal magnetic field structure. This is consistent with all the two-fluid FRC simulations we have performed so far, in which we have seen a toroidal field with a net zero toroidal magnetic flux. See Fig. 9 for details.

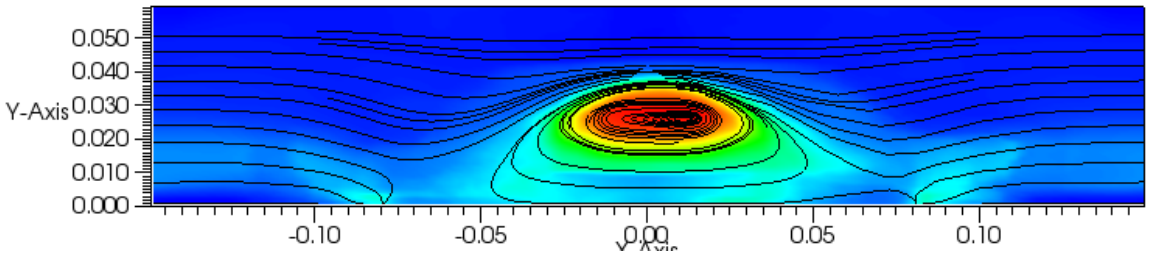

Figure 9. The plasma number density and the poloidal magnetic field streamlines are show at 3μs for the two-fluid relaxation problem. The plasma has contracted axially to form a new relaxed two-fluid equilibrium. The contraction has reduced the FRC length by half, thus indicating that ideal-MHD equilibrium is far from being a two-fluid equilibrium.

VI. Dense Plasma Focus

A recent application of Nautilus was to the simulation of a Dense Plasma Focus as a compact short-pulse (10 – 20 ns) neutron source. A dense plasma focus (DPF) is a machine that produces, by electromagnetic acceleration and compression, a short-lived pinch plasma that is hot and dense enough to produce intense radiation and neutrons. The plasma focus is similar to the high-intensity plasma gun, which ejects plasma in the form of a plasmoid, without pinching it. DPFs are being investigated around the world as neutron source as well as a fusion energy concept. Furthermore, the concept is very closely related to the magneto-plasma dynamic (MPD) thruster. The geometry of the device is simple: a truncated coaxial plasma accelerator is used to accelerate a current sheet down a coaxial tube. At the end of the coax the plasma assembles into a pinch where fusion reactions briefly occur. One distinguishing feature of DPFs as compared to Z-pinches is that the fusion reactions are largely non-thermonuclear. One relies on small scale sausage instability to drive ion beams in the plasma which results in beam-beam fusion.

An example of our effort is show in Figure 10, which shows the plasma density during the formation process. The plasma accelerates down the coaxial tube, eventually collapsing to the axis forming a Z-pinch. Due to the $1/r$ dependence of the toroidal magnetic field, the foot of the current sheet gets pushed further out than the top, which eventually leads to a longer formation time for the pinch than desired. One outcome of this is that the achieved neutron pulse is much longer than optimum, reducing the utility of this device to detect IEDs.

VII. Conclusions

In this paper we have presented an overview of Nautilus and shown results from a series of simulations of Field Reversed Configurations (FRCs) and Dense Plasma Focus (DPF) devices. Each application shows the need to cap-

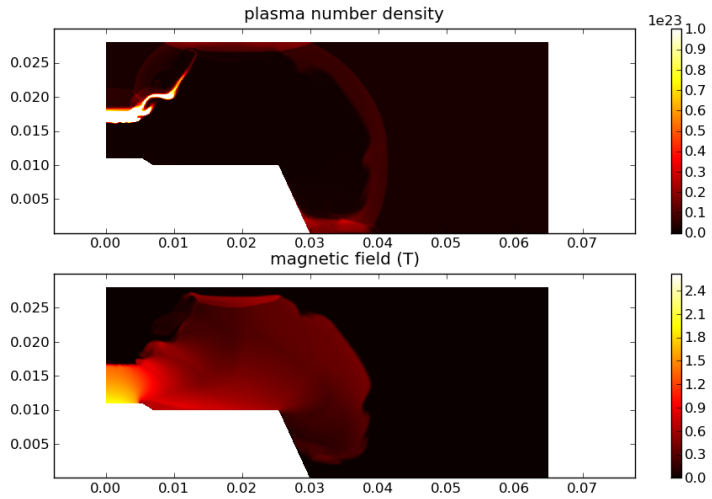

Figure 10. Dense plasma focus modeling using Nautilus. These simulation were performed by coupling an external pulse power system, modeled as a RLC circuit, with ideal MHD equations. The coupling of the RLC circuit to the plasma is achieved via inductance in the pinch, which is in fed back, at every time step, into the circuit model. The upper panel shows the number density and the lower panel the magnetic field. The formation of the on-axis pinch is clearly seen and this leads to the production of fusion neutrons.

ture the detailed physics of the underlying plasma processes and the need for accurate numerical methods that can resolve vacuum regions and different time and space scales. Continuing research on two-fluid physics will focus on implementing implicit methods for the electron fluid and the electromagnetic fields.

References

[1]Paul M. Bellan. *Spheromaks*. Imperial College Press, 2000.

[2]Elena V. Belova, Ronald C. Davidson, Hantao Ji, and Masaaki Yamada. Kinetic effect on the stability properties of field-reversed configurations. i. linear stability. *Physics of Plasmas*, 2003.

[3]Edward J. Cramana. Derivation of implicit difference schemes by the method of differential approximations. *Journal of Computational Physics*, 96:484–493, 1991.

[4]A. Hakim and U. Shumlak. Two-fluid physics and field-reversed configurations. *Physics of Plasmas*, 14:055911, 2007.

[5]Ammar Hakim, John Loverich, and Uri Shumlak. A high resolution wave propagation scheme for ideal two-fluid plasma equations. *Journal of Computational Physics*, 219, 2006.

[6]Ammar H. Hakim. Extended MHD modelling with the ten-moment equations. *Journal of Fusion Energy*, 27, 2008.

[7]A. Ishida, H Momota, and L.C. Steinhauer. Variational formulation for a multifluid flowing plasma with application to internal tilt mode of a field-reversed configuration. *Physics of Fluid*, 31(10):3024–3034, 1988.

[8]Andrei G. Kulikoviskii, Nikolai V. Pogorelov, and Andrei Yu. Semenov. *Mathematical Aspects of Numerical Solutions of Hyperbolic Systems*. Chapman and Hall/CRC, 2001.

[9]John Loverich and Uri Shumlak. A discontinuous galerkin method for the full two-fluid plasma model. *Computer Physics Communications*, 169, 2005.

[10]Richard D. Milroy and J.U Brackbill. Toroidal magnetic field generation during compact toroid formation in a field reversed theta pinch and a conical theta pinch. *Physics of Fluids*, 29(4), 1986.

[11]U. Shumlak and J. Loverich. Approximate Riemann Solver for the Two Fluid Plasma Model. *Journal of Computational Physics*, 187:620–638, 2003.

[12]C. R. Sovinec, A. H. Glasser, T. A. Gianakon, D. C. Barnes, R. A. Nebel, S. E. Kruger, D. D. Schnack, S. J. Plimpton, A. Tarditi, M. S. Chu, and the NIMROD Team. Nonlinear magnetohydrodynamic simulations using high-order finite elements. *Journal of Computational Physics*, 195:355–389, 2004.

[13]L.C. Steinhauer and A.Ishida. Relaxation of two-species magnetofluid and application to finite-β flowing plasma. *Physics of Plasmas*, 5(7):2609–2622, 1998.

[14]Loren C. Steinhauer. Formalism for multi-fluid equilibria with flow. *Physics of Plasmas*, 6(7):2734–2741, 1999.

[15]Loren C. Steinhauer, Hideaki Yamada, and Akio Ishida. Two-fluid flowing equilibria of compact plasmas. *Physics of Plasmas*, 2001.

[16]K. Wira and Z.A. Pietrzyk. Toroidal field generation and magnetic field relaxation in a conical-theta-pinch-generated configuration. *Physics of Fluids B*, 2(3), 1990.

[17]Hideaki Yamada and Takayuki Katano. Stability formalism of a flowing two-fluid plasma. *Physics of Plasmas*, 10(4):1168–1171, 2003.

[18]Hideaki Yamada, Takayuki Katano, and Kazumi Kanai. Equilibrium analysis of a flowing two-fluid plasma. *Physics of Plasmas*, 2002.